

## RESEARCH ARTICLE

## Preparation of Ca-chitosan and application for *Chlorella vulgaris* flocculation

Changli Liang\*, Chang Su, Shuhui Ying, Yuqing Xia, Yaru Yang, Yirong Dai, Junhe Liu, Han Wang

School of Biological and Food Processing Engineering, Huanghuai University, Zhumadian, Henan, China.

Received: November 5, 2024; accepted: April 16, 2025.

*Chlorella vulgaris* (*C. vulgaris*) has emerged as a premium feedstock for health food and pharmaceuticals production. Flocculation represents a cost-effective technology for overcoming the harvesting challenges in large-scale cultivation of *C. vulgaris*. Although chitosan is an ideal green flocculant for microalgae harvesting, but high cost hinders its commercial application. The main objective of the study was to develop a modified chitosan through grafting Ca (II) onto chitosan and optimize its flocculation parameters for *C. vulgaris*. Comprehensive characterization of the prepared Ca-chitosan through scanning electron microscope – energy dispersive spectrometer (SEM-EDS), Fourier transform infrared spectrophotometer (FTIR), and X-ray diffraction (XRD) confirmed the successful grafted of Ca (II). The flocculation rate reached 96.12% under optimized conditions (pH: 8.5, Ca-chitosan: 5.5 mg/L, flocculation time: 80 minutes) recommended by Response Surface Methodology (RSM). The results indicated that the integration of calcium with chitosan enhanced the flocculation efficiency for *C. vulgaris* by their synergistic effect. These findings demonstrated that Ca-chitosan has potential application prospect for industrial *C. vulgaris* flocculation harvesting.

**Keywords:** flocculation; *Chlorella vulgaris*; Ca-chitosan; response surface methodology.

\*Corresponding author: Changli Liang, School of Biological and Food Processing Engineering, Huanghuai University, Zhumadian 463000, Henan, China. Email: [lclwind@163.com](mailto:lclwind@163.com).

### Introduction

*Chlorella vulgaris* (*C. vulgaris*) has been widely used as high-quality raw materials for production health food, animal feed, biofuels, and pharmaceuticals due to its rich in protein, lipids, carbohydrates, pigments, vitamins, and minerals [1, 2]. However, the lack of cost-effective technique for microalgae harvesting remains a major bottleneck in large-scale production. Current harvesting cost accounts for approximately 20 – 30% of total microalgae biomass production costs due to their small cell size, stable suspension, and low biomass concentration [3, 4].

Microalgae harvesting methods primarily include filtration, centrifugation, flocculation, and membrane filtration [5, 6]. Among these techniques, flocculation stands out as a cost-effective and green approach for large-scale microalgae harvesting [7]. Current flocculation strategies mainly include self-flocculation, addition of multivalent cations such as ammonium sulfate, ferric sulfate, and ferric chloride, use of organic polymer like chitosan and polyelectrolytes, and application of bioflocculant [8]. Self-flocculation refers to the spontaneous aggregation of microalgae, which is regarded as an eco-friendly and efficient method of microalgae harvesting. However, few microalgae

species exhibit the capability, which limits its practical application [8]. Chemical flocculation microalgae by using multivalent cations or synthetic polymers demonstrates high flocculation efficiency, but the residual flocculants may contaminate the biomass and therefore limit their application in food production [8, 9]. Although bioflocculation has been proven to be effective and environmentally benign, but the adding of bioflocculant can pose possible potential contamination result from alter biomass composition [7, 10]. Chitosan, a cationic biopolymer derived from chitin deacetylation, has emerged as a promising flocculant for microalgae harvesting due to its inherent advantages of non-toxicity, biodegradability, and biocompatibility [11, 12]. Fraid *et al.* found that the optimal flocculation efficiency of *Nannochloropsis* sp by chitosan reached 93% at pH 9.0 with 100 mg/L chitosan [13]. However, the efficiency of marine diatom *Chaetoceros muelleri* flocculation by using chitosan was below 20% in acidic and slightly acidic pH conditions (pH 4.0 - 6.5) [12]. Economic analyses further indicated the limitations of *Chlorella vulgaris* flocculation by using chitosan. The cost of dry *C. vulgaris* biomass per ton for chitosan was 10 to 100 folds of conventional inorganic coagulants like aluminum sulfate and ferric chloride, which mainly attributed to its poor efficiency as 200 mg/L for 62% recovery [4]. These technical and economic constraints including pH-dependent performance instability, high reagent consumption, and high cost currently hinder chitosan's industrial-scale implementation in microalgae harvesting. Recent advancements in chitosan-based flocculation strategies focus on optimizing harvesting efficiency while reducing reagent consumption. For *Chlorella vulgaris*, supplementation with  $\text{FeCl}_3$  and  $\text{Al}_2(\text{SO}_4)_3$  enhanced chitosan flocculation efficiency by 57% and 24%, respectively [4]. In a comprehensive comparative analysis, Loganathan *et al.* evaluated the efficiency of mono- versus dual-flocculant systems for marine microalgae harvesting from seawater [10]. Remarkably, the chitosan-alum combination (1 ppm of chitosan + 10 ppm of

alum) achieved 97.6%, which was far higher than the maximum efficiency of 90.9% with 20 ppm chitosan. Our previous study demonstrated that the adjustment of pH using calcium hydroxide not only effectively improved *C. vulgaris* flocculation, but also significantly reduced chitosan dose [14]. These findings demonstrated that metal-chitosan combined application could effectively improve microalgae flocculation and simultaneously reduce the consumption of chitosan due to their synergistic action.

Crosslinking of metal ions with chitosan by complexation has been proved to effectively promote the adsorption capacity of chitosan for heavy metal ions from wastewater [15, 16]. However, few studies have investigated the crosslinking of chitosan with metal ions and its subsequent application for flocculating microalgae. This study synthesized a novel Ca-chitosan complex through ionotropic crosslinking of chitosan with  $\text{Ca}^{2+}$  ions to leverage their synergistic interactions for enhanced microalga flocculation and assessed its efficacy for *C. vulgaris* flocculation harvesting. Response surface methodology (RSM) was employed to systematically optimize critical parameters governing the flocculation process. This work provided theoretical and technological guidance for the modification of chitosan to prepare efficient chitosan base flocculants that could be used in the harvesting of microalgae.

## Materials and methods

### Cultivation of *C. vulgaris*

*C. vulgaris* used in the study was provided by Jiangxi Microalgae Cultivation and Further Processing Engineering Technology Center (Ruijin, Jiangxi, China). *C. vulgaris* was cultured in 600 mL modified BG-11 medium containing 0.8 g of urea, 0.25 g of  $\text{KH}_2\text{PO}_4$ , 0.205 g of  $\text{MgSO}_4 \cdot 7\text{H}_2\text{O}$ , 0.1 g of KCl, 0.026 g of  $\text{CaCl}_2 \cdot 2\text{H}_2\text{O}$ , and 0.018 g of  $\text{FeSO}_4 \cdot 7\text{H}_2\text{O}$  in 1 L of distill water and a GXZ-280A-LED illumination incubator (Ningbo Jiangnan Instrument Factory, Ningbo, Zhejiang, China) at  $30 \pm 1^\circ\text{C}$  and 12:12 h light/dark cycle at a light intensity of 5,800 lx.

**Table 1.** BBD matrix and the results of flocculation rate optimization.

Run	pH (A)	Ca-chitosan concentration (mg/L) (B)	Flocculation time (h) (C)	Flocculation reate (%)	
				Measured	Predicted
1	8.00	3.00	80.00	85.67	85.40
2	9.00	3.00	80.00	96.80	96.57
3	8.00	8.00	80.00	87.41	87.64
4	9.00	8.00	80.00	95.70	95.97
5	8.00	5.50	40.00	80.80	81.11
6	9.00	5.50	40.00	91.36	91.64
7	8.00	5.50	120.00	87.67	87.39
8	9.00	5.50	120.00	96.68	96.37
9	8.50	3.00	40.00	89.37	89.32
10	8.50	8.00	40.00	94.25	93.71
11	8.50	3.00	120.00	97.85	98.39
12	8.50	8.00	120.00	95.60	95.65
13	8.50	5.50	80.00	95.70	95.52
14	8.50	5.50	80.00	94.84	95.52
15	8.50	5.50	80.00	95.87	95.52
16	8.50	5.50	80.00	95.27	95.52
17	8.50	5.50	80.00	95.90	95.52

### Preparation of Ca-chitosan

Ca-chitosan was prepared by adding 8 g of chitosan (Shanghai Shifeng Biological Science and Technology Co., Ltd., Shanghai, China) into 100 mL saturated calcium chloride solution and stirring at 150 rpm for 1 hour before being filtrated and lyophilized to obtain solid Ca-chitosan.

### Single factor experiments

Single-factor experiments were conducted at sequent flocculation parameters including solution pHs at 7.0, 7.5, 8.0, 8.5, 9.0, Ca-chitosan concentrations of 1, 3, 5, 7, 10 mg/L, and flocculation time of 5, 10, 20, 40, 90, 120, 180 minutes. The initial OD<sub>680</sub> of *C. vulgaris* solution was adjusted to about 1.0 with deionized water. The pH values were adjusted to the set values used 0.1 M HCl or 0.1 M Ca(OH)<sub>2</sub>. Flocculation experiments were conducted in 30 mL of *C. vulgaris* solution. After stirring for 3 min, the solution was transferred into 30 mL graduated test tube, and settlement flocculation for the set time.

### Response surface methodology

The optimal range for the flocculation variables Ca-chitosan concentration, solution pH, and flocculation time were selected based on the results of single factor experiments. 17 experimental runs were performed with 5 replicates at the center of the design by Box–Behnken design (BBD). The experimental design matrix in coded and uncoded units were shown in Table 1. Flocculation rate (%) was determined through measuring the OD value at 680 nm of the supernatant taken from the middle of *C. vulgaris* suspension by UV 6000 spectrophotometer (Shanghai Leewen Scientific Instrument, Shanghai, China) before and after flocculation and was calculated as follows.

$$\text{Flocculation rate (\%)} = \frac{\text{OD}_{680i} - \text{OD}_{680f}}{\text{OD}_{680i}} \times 100 \quad (1)$$

### Characterization

Surface morphology of chitosan and Ca-chitosan sample was recorded by MLA650F field emission scanning electron microscope (FEI, Thermo Fisher Scientific, Richardson, Texas, USA). The elemental composition was detected using QUANTAX Energy Dispersion spectrometer (Rheinstetten, Bruker, Germany). Infrared

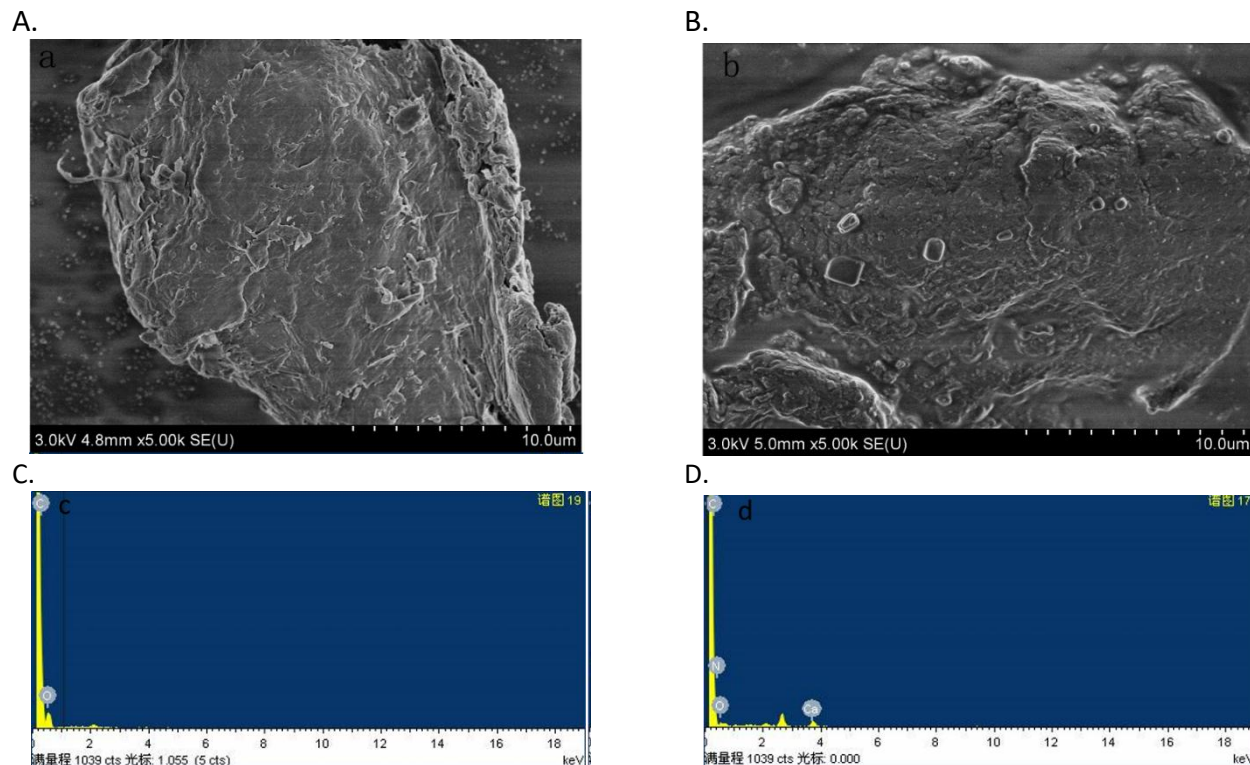


Figure 1. SEM spectra of chitosan (A) and Ca-chitosan (B), EDS spectra of chitosan (C) and Ca-chitosan (D).

spectra of chitosan and Ca-chitosan were recorded in the range of 4,000 – 800/cm using a Nicolet iS5 Fourier Transform Infrared spectrometer (FTIR) (Thermo Fisher Scientific, Waltham, Massachusetts, USA). The powder X-ray diffraction (XRD) measurements were performed using an Empyrean diffractometer (PANalytical Ltd., Netherlands).

### Statistical analysis

Design-Expert 8.06 software (Stat Ease Inc., Minneapolis, MN, USA) was used to estimate the pure error sum of squares and flocculation rate. The regression model and its accuracy and fitness were evaluated by analysis of variance (ANOVA). Origin 2018 (OriginLab Corporation, Northampton, Massachusetts, USA) was employed for the statistical analysis of this study. The results were presented as the mean values of triplicated experimental results under identical conditions.

## Results and discussion

### Characterization

To verify whether the Ca (II) was successfully grafted on chitosan, the chitosan and the Ca-chitosan were characterized by scanning electron microscope – energy dispersive spectrometer (SEM-EDS), XRD, and FTIR analysis. The results showed that the surface of chitosan was sheeted, while some rectangular and round crystalloid substances were found on the surface of Ca-chitosan (Figure 1A and 1B). EDS spectra revealed that the Ca (II) was grafted onto chitosan, and the Ca content on the surface of Ca-chitosan accounted for 2.84% (weight percent) (Figure 1C and 1D). The result confirmed the successfully grafted of Ca (II) onto chitosan. XRD was carried out to evaluate the phase and structure of chitosan and Ca-chitosan. Two characteristic diffraction peaks of chitosan were observed at 12° and 20° in the XRD spectrum of chitosan, respectively (Figure 2) [17]. In the spectra of Ca-chitosan, the diffraction peak at 20° was distinct

weakening, which should be due to the hydrogen bond between molecules in chitosan being disrupted after chelation of Ca and forming an amorphous structure [18]. The distinct crystal diffraction peaks of  $\text{CaCl}_2 \cdot (6\text{H}_2\text{O})$  were found in the spectrum of Ca-chitosan. XRD analysis confirmed that Ca was grafted onto chitosan.

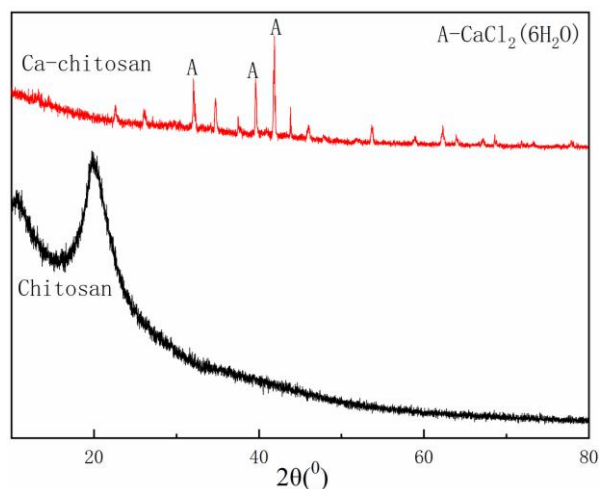


Figure 2. XRD spectra of chitosan and Ca-chitosan.

The FTIR spectra of chitosan and Ca-chitosan demonstrated that, in the spectra of chitosan, a broad band at around  $3,415/\text{cm}$  was assigned to the overlapped stretching vibrations of hydroxyl/amine, while the peak at  $1,639/\text{cm}$  was the distinguished stretching vibration of amide carbonyl band [19]. The stretching vibration of  $-\text{COO}-$  (symmetric),  $-\text{C-N}-$ , and  $-\text{C-O}-$  appeared at  $1,384/\text{cm}$ ,  $1,329/\text{cm}$ , and  $1,078/\text{cm}$ , respectively (Figure 3) [20]. Compared with chitosan, the amine peaks became sharp and negative shifted in the FTIR spectrum of Ca-chitosan. The overlapped stretching vibrations of hydroxyl peak and amine peak both sharpened and negative shifted to  $3,409/\text{cm}$  and  $1,597/\text{cm}$ , respectively. The negative shift of amide peaks of the amide groups on chitosan should be due to the coordination of Ca with the Ca being chemically adsorbed onto chitosan [20]. The peaks of  $-\text{COO}-$  (symmetric) at  $1,381/\text{cm}$  and  $-\text{C-N}-$  stretching vibration at  $1,327/\text{cm}$  both became stronger after Ca was grafted onto

chitosan. The shifted from  $1,078/\text{cm}$  to  $1,089/\text{cm}$  after grafted Ca indicated  $-\text{C-O}-$  groups took part in the adsorption. The results were consistent with previous report that also revealed some significantly changes happened in the  $-\text{N-H}-$  and  $-\text{C-N}-$  stretching vibration peaks of chitosan-cellulose beads after adsorption of  $\text{Cu(II)}$  [21]. The analysis of FTIR confirmed that the hydroxyl, carboxyl, and amide groups of chitosan took part in the chemical adsorption of  $\text{Ca(II)}$  onto chitosan. The analysis of SEM-EDS and XRD all confirmed that the Ca was grafted onto chitosan, and FTIR analysis confirmed that the graft was chemical adsorption.

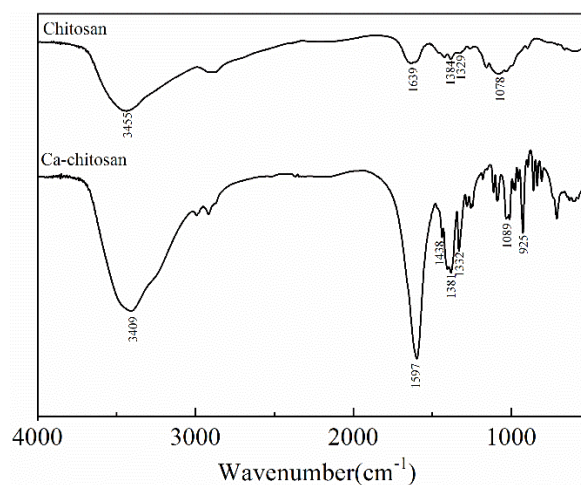
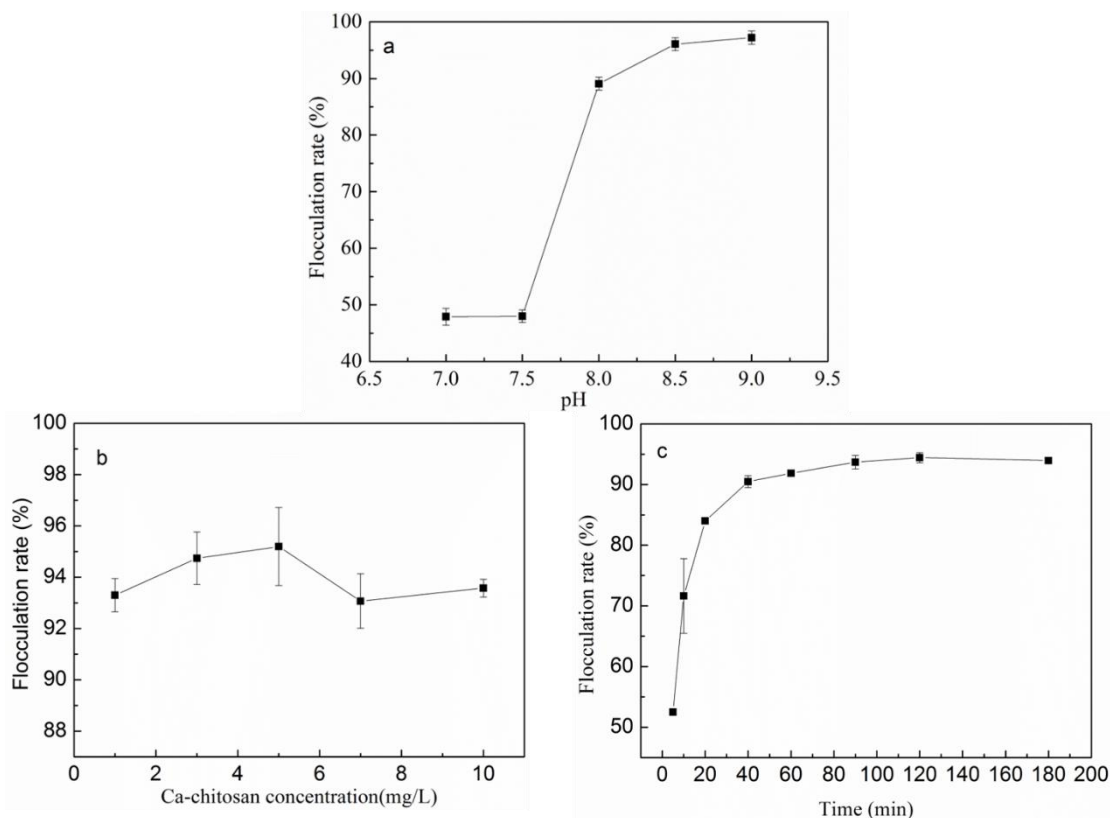


Figure 3. FTIR spectra of chitosan and Ca-chitosan.

### Single-factor experiment

*C. vulgaris* was flocculated with 5 mg/L Ca-chitosan in different pHs for 1 hour to evaluate the influence of pH on the flocculation behaviors. The results showed that the flocculation rate was less than 50% when pH was lower than 8.0, and then it increased rapidly from 48% to 89.1% when the pH was increased from 7.5 to 8.0 (Figure 4a). The increase rate was then slowed down over the pH interval of 8.0 to 9.0. The result was consistent with the study of Spilling *et al.* that the efficiency of flocculation microalgae by chitosan increased with the increase of pH in the interval of 6.5 to 8.2 [22]. Therefore, pH 8.5 was selected in the flow-up experiments.



**Figure 4.** Effect of pH (a), Ca-chitosan concentration (b), and flocculation time (c) on the flocculation performance of *C. vulgaris*.

Preliminary experiments demonstrated that the flocculation rate was higher than 90% when Ca-chitosan concentration was higher than 1 mg/L. The result confirmed that the Ca-chitosan was far more efficient than chitosan, indicating that there was synergistic action of Ca and chitosan. Therefore, the effect of Ca-chitosan concentration (1 - 10 mg/L) on the flocculation rate of *C. vulgaris* was studied. The results showed that the flocculation rate recorded an oscillating trend of 93.1 - 95.2% in the concentration range studied with the maximum flocculation rate of 95.2% being achieved at 5 mg/L (Figure 4b). The flocculation rate decreased slowly when the concentration was higher than 5 mg/L, which was mainly because excess calcium chitosan caused some *C. vulgaris* cells to have a positive surface charge and lead to restabilization of the suspension through electrostatic repulsion [23]. Therefore, 5 mg/L Ca-chitosan was chosen in the following experiment. The flocculation rate increased quickly with the increase of

sedimentation time at the first 40 minutes, and more than 90% *C. vulgaris* was flocculated in the stage. It then increased slowly and reached equilibrium with the extension of flocculation, and the maximum flocculation rate reached 94.45% at 120 minutes (Figure 4c). The results were consistent with the research of Kumaran *et al.* that more than 90% of the marine diatom *Chaetoceros muelleri* was flocculated by using chitosan in the first 40 minutes, and no significant increase was observed with the extension of flocculation [12]. The results of this study might be because the aggregation of *C. vulgaris* through electrostatic attraction and bridging action that required sufficient time before reaching equilibrium. Therefore, more than 80 minutes and no longer than 120 minutes were required for the sufficient flocculation of *C. vulgaris*.

#### Response surfaces optimization

Ca-chitosan concentration, pH, and flocculation time were chosen as the variables, and the

**Table 2.** ANOVA of the fitted quadratic polynomial model of flocculation rate.

Source	Sum of squares	df	Mean square	F value	P value
Model significant	374.60	9	41.62	144.37	< 0.0001
pH (A)	190.03	1	190.03	659.12	< 0.0001
Ca-chitosan concentration (B)	1.34	1	1.34	4.64	0.0683
Flocculation time (C)	60.61	1	60.61	210.23	< 0.0001
AB	2.02	1	2.02	6.99	0.0332
AC	0.60	1	0.60	2.08	0.1921
BC	12.71	1	12.71	44.08	0.0003
A <sup>2</sup>	90.28	1	90.28	313.14	< 0.0001
B <sup>2</sup>	1.09	1	1.09	3.79	0.0926
C <sup>2</sup>	13.01	1	13.01	45.14	0.0003
Residual	2.02	7	0.29		
Lack of Fit	1.19	3	0.40	1.93	0.2662
Pure Error	0.82	4	0.21		
Cor Total	376.62	16			

flocculation parameters were optimized by RSM. The measured and predicted values of flocculation rates were shown in Table 1. A quadratic model was obtained by fitting the experimental data into Design-Expert 8.06. The model in terms of the coded factors was then determined to calculate the flocculation rate (%) of *C. vulgaris* as follows.

$$\text{Flocculation rate (\%)} = 95.52 + 4.87A + 0.41B + 2.75C - 0.71AB - 0.39AC - 1.78BC - 4.63A^2 + 0.51B^2 - 1.76C^2 \quad (2)$$

where A, B, and C were pH, Ca-chitosan concentration, and flocculation time, respectively. ANOVA test, regression coefficient estimate, and test of significance for flocculation *C. vulgaris* with Ca-chitosan were performed to evaluate the statistical significance. The results showed low *P* value and high *F* value of the proposed model ( $P < 0.0001$ ,  $F = 144$ ), which indicated that the proposed quadratic polynomial model was significant and suitable for the prediction of experimental data. Lack of fit (LOF) represents the difference between the model function and the real function. The model was considered significant when the *P* value was higher than 0.05, and the LOF as 0.266 in the study, which indicated that the model was suitable for the prediction of flocculation rate

(Table 2) [24]. Adequate precision is the ratio value of signal to noise, and the value larger than 4 is considered as desirable [25]. In the present study, the adequate precision value of 41.961 was far larger than 4, which confirmed the consistency of the predicted and measured values. The  $R^2$  coefficient represents the proportion of the total variation in the response predicted by the model, indicating ratio of sum of squares due to regression to total sum of squares. The closer of the correlation coefficient ( $R^2$ ) to 1 is desirable and a reasonable agreement with adjusted  $R^2$  is necessary [26]. The results showed that the  $R^2$  value of 0.9946, adjusted  $R^2$  of 0.9878, and predicted  $R^2$  of 0.9459 highlighted the high correlation between experimental and predicted values. The predicted values were very close to the measured values (Table 1), which confirmed that the model could be used to predict the flocculation rate of *C. vulgaris*. The results demonstrated that all residues lied on and near to the fitted straight line (Figure 5), which confirmed the constancy of the variance and normal distribution of data. The normal probability plot further confirmed the good agreement between the predicted and experiment data. The results showed significant influences of pH and flocculation time on the flocculation rate of *C. vulgaris* ( $P < 0.05$ ), while Ca-chitosan concentration did not show



significant influence ( $P > 0.05$ ). Further, the interaction of pH and Ca-chitosan concentration demonstrated significant effect on the flocculation rate of *C. vulgaris* ( $P < 0.05$ ), while the interaction of Ca-chitosan concentration and the flocculation time also demonstrated the significant effect ( $P < 0.05$ ).

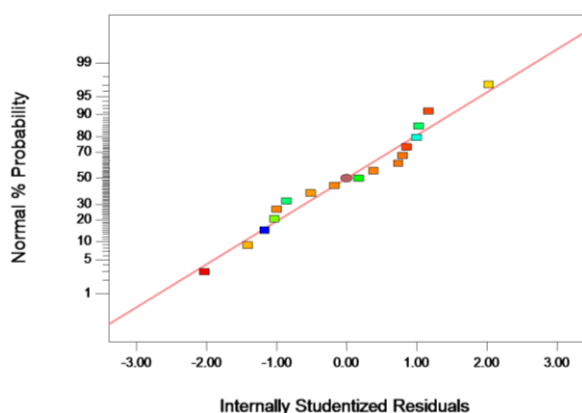


Figure 5. Normal probability plot of residuals.

Three-dimensional (3D) surface response plots and two-dimensional contour plots can be used to determine the interaction between the variables and their significance in the response [27]. The flocculation rate first increased with the increase of pH from 8.0 to 8.6 and reached the maximum value of 96.1% and then slightly decreased with the pH increased further (Figure 6a and 6c). Similar results were found in some studies on the flocculation of microalgae by using chitosan [13, 28]. The flocculation rate kept increasing with the increase of pH might be because the higher pH could provide more positive charge to neutralize the negative charge on the microalgae cell surface and resulted in the aggregation of *C. vulgaris* through electrostatic attraction [29]. The slight decrease in the elevated pH levels might be attributed to the excessive positive charge that could induce the electrostatic repulsion among *C. vulgaris* cells and consequently reduce aggregation tendency. The influence of pH on *C. vulgaris* flocculation was consistent with that in single factor experiment. The flocculation rate kept increasing

with the increase of Ca-chitosan concentration from 3 to 8 mg/L (Figure 6a and 6e). However, the influence was not significant as that of pH value. The promotion effect of Ca-chitosan concentration was indistinctive because the flocculation rate maintained at a high level in the studied range. Similar results were found in the flocculation of marine diatom *Chaetoceros muelleri* with chitosan [12]. Compared the photos of raw *C. vulgaris* with that flocculated by Ca-chitosan confirmed the formation of cells flocs during *C. vulgaris* flocculation (Figure 7). Ca-chitosan induced the entrapment and bridging of *C. vulgaris* cells. The grafted of Ca could stimulate *C. vulgaris* cells aggregation to form bigger flocs by neutralization the negative charge of cells [30]. Flocculation time showed a distinct influence on *C. vulgaris* flocculation by Ca-chitosan. The flocculation rate increased from about 84% to 98% along with flocculation time increased from 40 to 120 minutes (Figure 6b and 6e). Similar results were found in the flocculation of *Chaetoceros muelleri* by chitosan and *C. vulgaris* flocculated by using chitosan [12, 31]. The increased flocculation rate with the increase of flocculation time might be because the break of the steady state by charge neutralization and the bridging of small cells to form bigger flocs both require enough time before it reached the balance. The extension of time could not distinctly promote the flocculation of *C. vulgaris* when it reached equilibrium. The elliptical contour plot represents the significant interaction between independent variables [32]. The results showed that there were indistinct interactions between the variables for no contour plots exhibited elliptical shape (Figure 6b, 6d, and 6f). The results confirmed the analysis results of ANOVA.

The predicted flocculation rate was 95.52% under the optimized flocculation conditions that were pH of 8.5, Ca-chitosan concentration of 5.5 mg/L, and flocculation time of 80 minutes. Three verification tests were carried out to evaluate the precision of the model with the measured flocculation rate of 96.12%, which was consistent with the predicted value and confirmed the



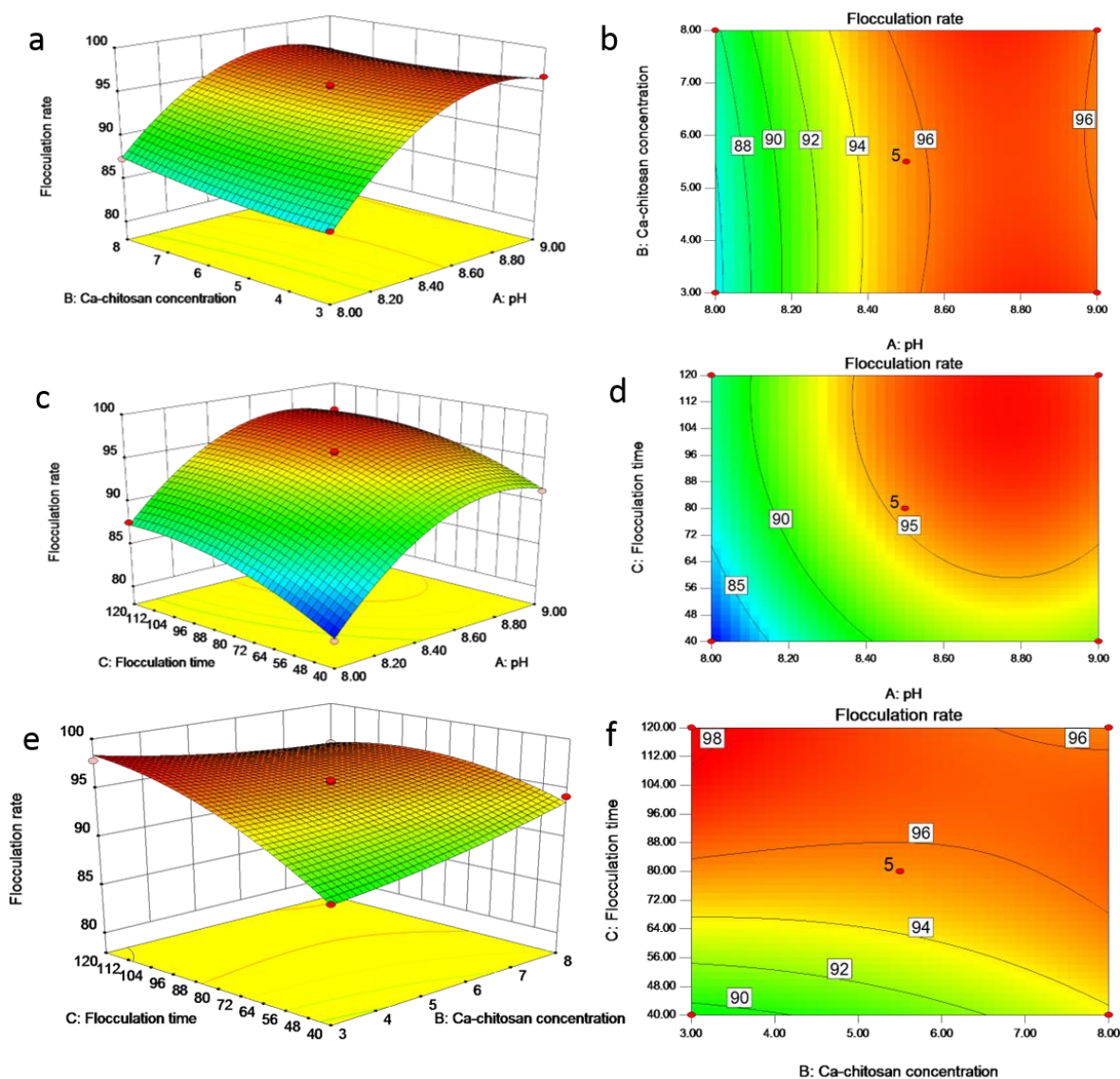


**Figure 6.** Response surfaces and their corresponding contour plots for flocculation rate of *C. vulgaris* as a functional of pH and flocculation time (a, b), pH and Ca-chitosan concentration (c, d), Ca-chitosan concentration and flocculation time (e, f).

validity of the proposed model. Previous research reported that the flocculation rate of *Scenedesmus* was lower than 10% when the chitosan concentrations were in the range of 0 to 20 mg/L [33]. Cai *et al.* also reported that the flocculation rate of *Scenedesmus* all lower than 30% when quaternary ammonium chitosan concentrations were in the range of 0 to 20 mg/L, while the flocculation rate was higher than 95% when the combination use of 8 mg/L quaternary ammonium chitosan and 16 mg/L xanthan gum [34]. The maximum flocculation rate 87.3% was

achieved under the microalgae flocculation by 30 mg/L chitosan. The relationship between chitosan concentration and *Chlorella vulgaris* biomass revealed that 250 mg/L, 125 mg/L, and 50 mg/L chitosan were needed to insure the flocculation rate no lower than 90% when the biomass concentrations were 1.2 g/L, 0.8 g/L, and 0.5 g/L, respectively [31]. More than 99% of marine diatom *Chaetoceros muelleri* could be flocculated by 80 mg/L chitosan at alkaline condition [12]. Vu *et al.* found that the flocculation rate of *C. vulgaris* was around 20%

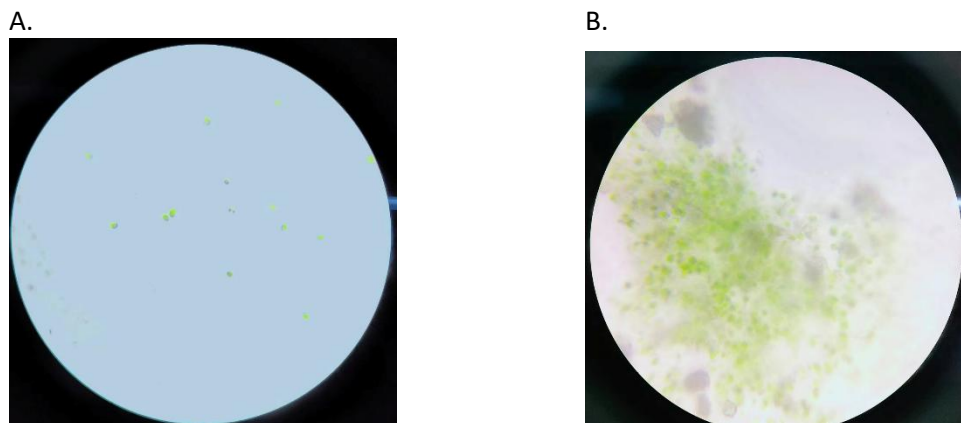


Figure 7. Photos of raw *C. vulgaris* (A) and flocculation by Ca-chitosan (B).

and 60% by using 40 mg/L and 200 mg/L chitosan, respectively [4]. The flocculation performance of *C. vulgaris* by using Ca-chitosan in this study demonstrated obvious advantages in comparison with the previous studies.

### Conclusion

In this study, calcium-chitosan was prepared by chemical adsorption of Ca(II), hoping that the modified chitosan could exert the synergistic effect of Ca(II) and chitosan to flocculate *Chlorella vulgaris*. The results of XRD and SEM-EDS both confirmed the successful graft of Ca(II) onto chitosan. FTIR analysis confirmed that the Ca(II) was chemical adsorbed by the hydroxyl, carboxyl, and amide groups of chitosan. The influence of Ca-chitosan concentration on the flocculation confirmed that Ca-chitosan was an efficient flocculant for *C. vulgaris*. Flocculation rate of *C. vulgaris* by using Ca-chitosan reached 96.12% under the optimal conditions proposed by RSM, indicated that the modified chitosan by Ca(II) effectively improved the performance of chitosan in the flocculation of *C. vulgaris*. The results of this research provided useful information for the application of Ca-chitosan in the flocculation harvesting of microalgae and guide for the exploring of efficient chitosan base flocculants.

### Acknowledgements

This work was supported by the Primary Research & Development Plan of Henan Province (Grant No. 23111320300) and the Joint Fund for Science and Technology Research and Development of Henan Province (Grant No. 242103810011).

### References

1. Khoo KS, Chia WY, Chew KW, Show PL. 2021. Microalgal-bacterial consortia as future prospect in wastewater bioremediation. *Environmental management and bioenergy production*. *Indian J Microbiol*. 3:262-269.
2. Oliveira C, Rabello D, Daniel NM. 2019. Biomass production and harvesting of *Desmodesmus subspicatus* cultivated in flat plate photobioreactor using chitosan as flocculant agent. *J Appl Phycol*. 31:857-866.
3. Show PL, Tan JS, Lee SY, Chew KW, Ho SH. 2020. A review on microalgae cultivation and harvesting, and their biomass extraction processing using ionic liquids. *Bioeng*. 11(1):116-129.
4. Vu HP, Nguyen LN, Lesage G, Nghiem LD. 2020. Synergistic effect of dual flocculation between inorganic salts and chitosan on harvesting microalgae *Chlorella vulgaris*. *Environ Technol Innov*. 17:100622.
5. Kadir WNA, Lam MK, Uemura Y, Lim JW, Kiew PL, Lim S, *et al*. 2021. Simultaneous harvesting and cell disruption of microalgae using ozone bubbles: Optimization and characterization study for biodiesel production. *Front Chem Sci Eng*. 15(5):1257-1268.
6. Leite LDS, Hoffmann MT, Daniel LA. 2019. Coagulation and dissolved air flotation as a harvesting method for microalgae cultivated in wastewater. *J Water Process Eng*. 32:100947.
7. Shitanaka T, Fujioka H, Khan M, Kaur M, Du ZY, Khanal SK, *et al*. 2024. Recent advances in microalgal production, harvesting,

- prediction, optimization, and control strategies. *Bioresource Technol.* 391:129924.
8. Malik S, Khan F, Atta Z, Habib N, Haider MN, Wang N, *et al.* 2020. Microalgal flocculation: Global research progress and prospects for algal biorefinery. *Biotechnol Appl Biochem.* 67(1):52-60.
  9. Rinanti A, Purwadi R. 2018. Harvesting of freshwater microalgae biomass by *Scenedesmus* sp. as bioflocculant. *IOP Conference Series: Earth and Environmental Science.* 106:012087.
  10. Loganathan K, Saththasivam J, Sarp S. 2018. Removal of microalgae from seawater using chitosan-alum/ferric chloride dual coagulations. *Desalination.* 433:25-32.
  11. Dai D, Qv MX, Liu DY, Tang CM, Wang W, Wu QR, *et al.* 2023. Structural insights into mechanisms of rapid harvesting of microalgae with pH regulation by magnetic chitosan composites: A study based on E-DLVO model and component fluorescence analysis. *Chem Eng J.* 456:141071.
  12. Kumaran J, Singh ISB, Joseph VJ. 2021. Effective biomass harvesting of marine diatom *Chaetoceros muelleri* by chitosan-induced flocculation, preservation of biomass, and recycling of culture medium for aquaculture feed application. *J Appl Phycol.* 33(3):1605-1619.
  13. Farid MS, Shariati A, Badakhshan A, Anvaripour B. 2013. Using nano-chitosan for harvesting microalga *Nannochloropsis* sp. *Bioresource Technol.* 131:555-559.
  14. Liang CL, Yang YR, Xia YQ, Yuan WW, Chen J, Zheng ZF, *et al.* 2022. The optimization of *Chlorella vulgaris* flocculation harvesting by chitosan and calcium hydroxide. *Indian J Microbiol.* 62(2):266-272.
  15. He J, Lu YC, Luo GS. 2014. Ca(II) imprinted chitosan microspheres: An effective and green adsorbent for the removal of Cu(II), Cd(II) and Pb(II) from aqueous solutions. *Chem Eng J.* 244:202-208.
  16. Sun S, Wang A. 2006. Adsorption properties and mechanism of cross-linked carboxymethyl-chitosan resin with Zn(II) as template ion. *React Funct Polym.* 66(8):819-826.
  17. Lu X, Xu Y, Sun W, Sun Y, Zheng H. 2017. UV-initiated synthesis of a novel chitosan-based flocculant with high flocculation efficiency for algal removal. *Sci Total Environ.* 609:410-418.
  18. Sun Y, Zhu C, Sun W, Xu Y, Xiao X, Zheng H, *et al.* 2016. UV-initiated graft copolymerization of cationic chitosan-based flocculants for treatment of zinc phosphate-contaminated wastewater. *Ind Eng Chem Res.* 55:10025-10035.
  19. Ye NS, Xie AY, Shi PZ, Gao T, Ma JC. 2014. Synthesis of magnetite/graphene oxide/chitosan composite and its application for protein adsorption. *Mat Sci Eng C: Mat Biological App.* 45:8-14.
  20. Ding P, Li GY, Chen CM, Huang KL. 2011. Kinetics and mechanism of chelating reaction between chitosan derivatives with Ca(II). *J Coord Chem.* 64(8):1333-1343.
  21. Li N, Bai R. 2005. Copper adsorption on chitosan-cellulose hydrogel beads: Behaviors and mechanisms. *Separ Purif Technol.* 42:237-247.
  22. Spilling K, Seppälä J, Tamminen T. 2011. Inducing autoflocculation in the diatom *Phaeodactylum tricornutum* through CO<sub>2</sub> regulation. *J Appl Phycol.* 23:959-966.
  23. Wan C, Zhao XQ, Guo SL, Alam MA, Bai FW. 2013. Bioflocculant production from *Solibacillus silvestris* W01 and its application in cost-effective harvest of marine microalga *Nannochloropsis oceanica* by flocculation. *Bioresource Technol.* 135:207-212.
  24. Ghafari S, Aziz HA, Isa MH, Zinatizadeh AA. 2009. Application of response surface methodology (RSM) to optimize coagulation-flocculation treatment of leachate using poly-aluminum chloride (PAC) and alum. *J Hazard Mater.* 163(2-3):650-656.
  25. Shahadat M, Teng TT, Rafatullah M, Shaikh ZA, Sreekrishnan TR, Ali SW. 2017. Bacterial bioflocculants: A review of recent advances and perspectives. *Chem Eng J.* 328:1139-1152.
  26. Pishgar Z, Samimi A, Mohebbi-Kalhari D, Shokrollahzadeh S. 2020. Comparative study on the harvesting of marine *Chlorella vulgaris* microalgae from a dilute slurry using autoflocculation-sedimentation and electrocoagulation-flotation methods. *Int J Environ Res.* 14(6):1-14.
  27. Yaakob Z, Abdullah S, Takriff MS. 2019. Analysis of the elemental composition and uptake mechanism of *Chlorella sorokiniana* for nutrient removal in agricultural wastewater under optimized response surface methodology (RSM) conditions. *J Clean Prod.* 210:673-686.
  28. Sirin S, Trobajo R, Ibanez C, Salvadó J. 2012. Harvesting the microalgae *Phaeodactylum tricornutum* with polyaluminum chloride, aluminium sulphate, chitosan and alkalinity-induced flocculation. *J Appl Phycol.* 24(5):1067-1080.
  29. Lee SM, Choi HJ. 2015. Harvesting of microalgae species using Mg-sericite flocculant. *Bioproc Biosyst Eng.* 38(12):2323-2330.
  30. Alam MA, Vandamme D, Chun W, Zhao X, Foubert I, Wang Z, *et al.* 2016. Bioflocculation as an innovative harvesting strategy for microalgae. *Rev Environ Sci Bio.* 15(4):1-11.
  31. Zhu LD, Li Z, Hiltunen E. 2018. Microalgae *Chlorella vulgaris* biomass harvesting by natural flocculant: Effects on biomass sedimentation, spent medium recycling and lipid extraction. *Biotechnol Biofuels.* 11(1):183.
  32. Muralidhar R, Chirumamila R, Marchant R, Poonam S. 2001. A response surface approach for the comparison of lipase production by *Candida cylindracea* using two different carbon sources. *Biochem Eng J.* 9(1):17-23.
  33. Xu L, Cai Q, Liu X, Cai P, Tian C, Wu X, *et al.* 2023. Instantaneous and reversible flocculation of *Scenedesmus* via chitosan and xanthan gum complexation. *Bioresource Technol.* 390:129899.
  34. Cai Q, Gong S, Song K, Cai P, Tian C, Wang C, *et al.* 2021. Effective harvesting of *Scenedesmus* using quaternary ammonium chitosan and xanthan gum: Formation of mega flocs with oppositely charged polyelectrolytes. *J Clean Prod.* 329:129730.